Progress in soft X-ray and UV photocathodes

S.R. Jelinsky, O.H.W. Siegmund, and J.A. Mir
University of California
Space Sciences Laboratory
Berkeley, CA 94720

ABSTRACT

We present investigations on the improvements in quantum detection efficiency (QDE) of microchannel plate (MCP) detectors resulting from the application of various photocathode materials. Nine different photocathode materials were deposited and their QDE measured in the soft X-ray and UV region from 12Å to 1850Å. Four of these materials (CsCl, RbCl, RbI, BaCl) significantly enhance the QDE performance of bare MCP's, and five materials were proven unsatisfactory (AgCl, LiCl, LiI, LiF, MgBr). CsCl has very high (>90%) short wavelength QDE and both CsCl and RbI have UV QDE in the region of 40%. Our studies also include life testing of a KBr photocathode for a period of over 5 years. This shows good stability, and the angular response and photoemissive characteristics over time are described. The effects of long wavelength QDE activation of KBr by exposure to 2537Å photons are discussed.

Keywords: quantum detection efficiency, microchannel plate, photocathode

1.0 INTRODUCTION

The technique of enhancing the quantum detection efficiency of microchannel plate (MCP) detector systems by coating the top channel plate with a layer of photoemissive material has been well established over more than two decades[1,2]. An opaque photocathode material is deposited on the top of a MCP detector and incoming photons interact with the photocathode. Photoelectrons emitted by the photocathode inside the channels are accelerated into the MCP wall producing many secondaries, which are further multiplied by the MCP. The result is a charge avalanche in the MCP's with an overall charge multiplication often of $> 2 \times 10^7$. There are a number of known materials that have been proven useful as photocathodes in the soft X-ray and UV thus far, each with its own region of high efficiency. Future spacecraft instruments pose new challenges for cathode development, such as improvements in QDE, suppression of out of bandpass scattered radiation, better knowledge on the stability of cathode materials, better energy discrimination and coverage of wider wavelength ranges.

The materials for study were chosen on the basis of their band gap to electron affinity ratio, mass absorption coefficient, extent of hygroscopic behavior, and measured photoyield. For soft X-ray and UV cathodes, our model of QDE behavior is largely driven by the mass absorption coefficient, so we assume this to be a good indicator of general QDE trends. Our choice of photocathodes concentrated on the alkali halide materials which have small band gaps (E_g), and high E_g to electron affinity (E_a) ratios. Thus, the alkali halide materials typically have high QDE with highly structured QDE vs. energy dependencies, but they are unfortunately highly susceptible to water vapor deterioration. Our studies have revealed a few promising new photocathode materials as well as elimination other materials from further investigation.

2.0 PHOTOCATHODE FABRICATION

The photocathode materials were vacuum deposited directly onto the top MCP following well established procedures[3,4]. High purity (99.999%) (H_2O, OH, Oxide <100ppm) photocathode material was evaporated from a rectangular molybdenum boat by resistive heating in a vacuum system at 10^{-6}

0-8194-2196-0/96/$6.00

torr. Prior to deposition the material is heated behind a shutter to outgas any absorbed water, in some cases over 12 hours. The MCP's used are 36mm diameter, 12um pore, 40:1 L/D, with a 13 degree bias angle. During the evaporation, the MCP is rotated at 0.5 rev/sec, with the rotation axis aligned parallel to the channel axis. The alignment of the photocathode source with respect to the channel bias was optimized for improvements in QDE performance in the soft x-ray region or UV regions respectively.

The photocathode source, or boat, is typically aligned with between 10 degrees offset from the channel axis, to 3 degrees from the channel axis. The evaporation angle determines the cathode penetration depth into the channels, using a smaller evaporation angle results in a deeper penetration depth. The photocathode depositions resulted in photocathode thicknesses on the face of the MCP, or web thickness, between 7,000 and 17,000Å deep. The web thickness is determined by the change in weight of a witness sample and the deposition rate was determined by a quartz crystal monitor positioned close to the MCP. The cathode fabrication conditions for each of the photocathode materials we present, such as evaporation angle, deposition rate, and web thickness are listed in Table I.

Photocathode Material	Evaporation Rate (Å/s)	Angle (deg)	Thickness (Å)
AgCl	11	6	6,670
BaCl	3	2	8,700
CsCl	3	5	16,690
CsI	3	5	7,415
LiCl	3	9	8,210
LiF	3	2	14,660
LiI	3	6	5,780
MgBr	7	4	7,170
RbCl	11	4	7,730
RbI	11	6	9,240
RbI	3	6	10,975

Table I. Photocathode fabrication parameters used.

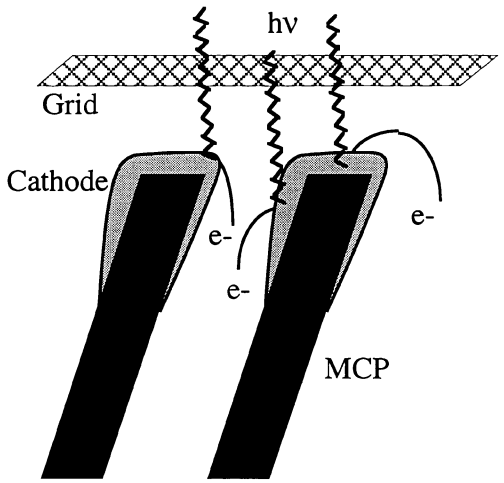

Figure 1. Schematic of an opaque cathode layer on an MCP with a photoelectron repeller grid.

The photocathodes were deposited on MCP's that were masked over one third of their area, thus preserving a bare area of the MCP. This enabled a direct comparison of the QDE measurements between photocathode and bare for each MCP. The bare MCP QDE values are reasonably stable and repeatable, so a bare QE measurement provides a reliable cross check of our measurement system.

3.0 MEASUREMENT CONFIGURATION

Once the MCP has been coated, it is then installed into a Z-stack MCP detector system[5], complete with a wedge-and-strip anode[6] for photon counting, imaging applications, then installed in a vacuum chamber for calibration. A 90% transmissive nickel mesh is mounted over the aperture of the detector to apply a retarding potential preventing the loss of front side emitted photoelectrons, thus greatly increasing the QDE[7]. A typical configuration for an opaque photocathode is shown in Fig. 1. In all the QDE measurements presented here, a retarding field of 15 Vmm^{-1} was applied. The QDE vs energy properties were measured in an ultra high vacuum of 10^{-6} torr with the MCP detector mounted on a four axis manipulator with a rotation stage. Monochromatic radiation was provided by an electron bombarded target X-ray source or by a gas discharge hollow cathode source in combination with a 1m grazing incidence monochromator. After corrections are made for the transmission of the retarding mesh and the contribution of the background radiation, then the absolute QDE's are derived from flux measurement comparisons with a reference standard. The choice of reference standard depends on wavelength

measured; there is a Manson soft x-ray proportional counter, a NIST ultraviolet windowless photodiode, or a NIST far ultraviolet windowed photodiode. In general, the accuracy of the absolute QDE measured is determined by the accuracy of the reference standards. The Manson proportional counter readings have a most probable error of 15% at wavelengths below 44Å. The NIST EUV photodiode has a most probable error of 15% between 44Å and 68Å, and 10% from 68Å to 1216Å. The NIST far ultraviolet photodiode has a most probable error of 10% from 1216Å to 2537Å.

The graze angle of the incident radiation with respect to the channel plate pores has an effect on the QDE of the MCP. This angular dependence on the QDE performance has been studied previously[2,8]. The QDE is at its minimum when the beam is parallel with the MCP pores, when there is essentially no reflection off the channel walls. The QDE then increases rapidly to a maximum as the beam approaches the critical graze angle of reflection. Then it drops off with increasing graze angle in due to a decline in the photoelectron escape probability. The QDE peaks at smaller angles for shorter wavelengths and at larger angles for longer wavelengths. In our studies of the improvements in QDE from photocathodes, the QDE measurements were made only at the optimal graze angle (to within 1 degree) for each wavelength. The optimal graze angle was measured to be ≈3° at 12Å wavelength, increasing to 5° between 44Å and 171Å, then 10° for wavelengths between 256 and 584Å, and finally 15° for all wavelengths measured greater than 584Å.

4.0 QUANTUM DETECTION EFFICIENCY RESULTS

The effectiveness of the photocathodes tested varied widely, some being quite good and others very poor. The best photocathodes were those closely related to others proven to have good performance. Some of the poor photocathodes were bad not because they had poor QDE, but rather because they were not stable to atmospheric conditions.

4.1. CsCl, RbI & RbCl photocathodes

Each photocathode was measured for QDE response as a function of angle and then measured for QDE as a function of wavelength. The QDE at the peak QDE angle is presented in the figures. This changes from ≈10° to the MCP pore axis at long wavelengths, to <5° at 44Å and below. The bare half of the MCP was also measured to provide a comparison.

CsCl QDE as a function of angle and wavelength are presented in Figures 2 and 3 respectively. CsCl has a band gap + electron affinity of ≈8.0eV, giving a photoemission threshold of ≈1550Å. It is hygroscopic, with a solubility of 160-260gm/cc, which would seem to indicate that it would be a difficult material to employ for devices requiring atmospheric exposure. We have found that the handling requirements for CsCl are much like those for CsI and, therefore, tolerable. Photoemission data[9] also indicates that CsCl should be a good photocathode material, with yields similar to CsI. The angular QDE response is much as expected, the width of the dip corresponding to the pore axis angle is narrower for shorter wavelengths illustrating the effect of grazing incidence reflection at short wavelength. The fairly rapid drop in QDE at angles >5° for 44Å light is indicative of the low photoelectron escape probability at this wavelength due to the low photoabsorption coefficient[10]. Meanwhile the peak in the QDE at ≈ 114Å correlates with the resonant peak in the absorption coefficient found at 105eV [10]. The attenuation length at this wavelength is small so that even at large incidence angles (Fig. 2) the photoelectrons can escape the cathode resulting in high QDE. The cutoff at about 1600Å is apparent in Figure 3, as is the 2 x bandpass QDE minimum at ≈800Å. Local maxima are found at ≈584Å and 1000Å , corresponding to one, and two photoelectron emission respectively. CsCl has slightly better overall QDE than CsI (see Fig. 8), but has a shorter wavelength photoemission threshold.

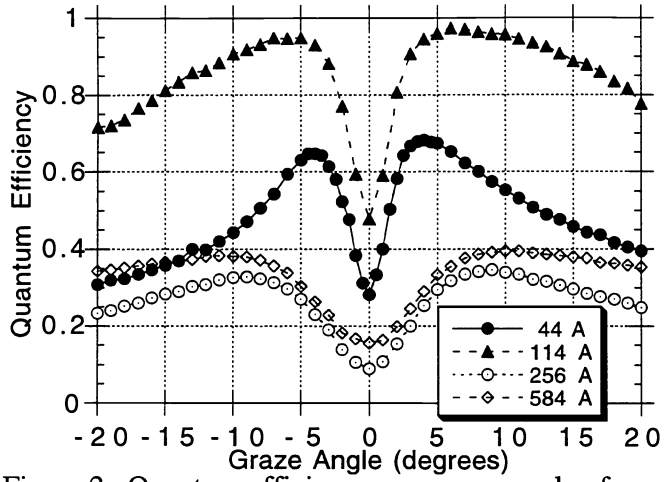

Figure 2. Quantum efficiency v.s. graze angle of incidence to the MCP pores for CsCl.

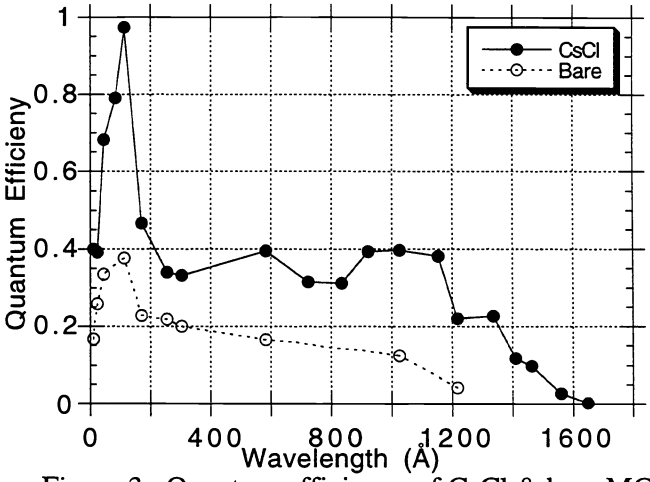

Figure 3. Quantum efficiency of CsCl & bare MCP measured at the peak angle, v.s. wavelength.

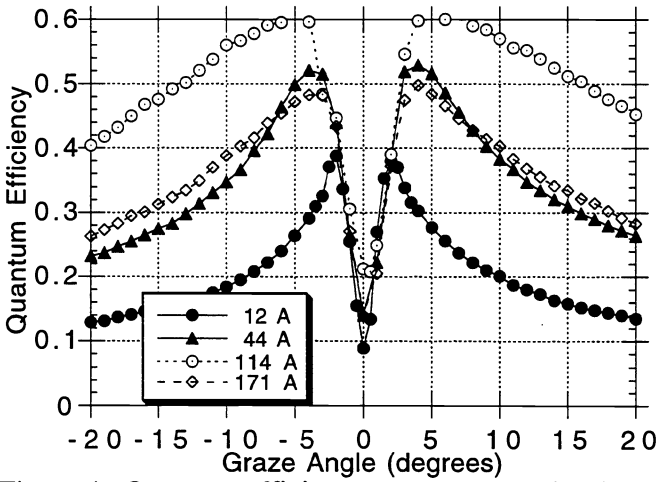

Figure 4. Quantum efficiency v.s. graze angle of incidence to the MCP pores for RbI.

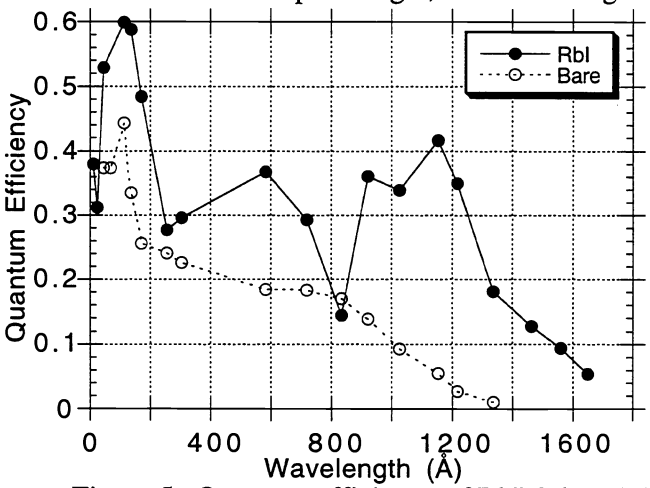

Figure 5. Quantum efficiency of RbI & bare MCP measured at the peak angle, v.s. wavelength.

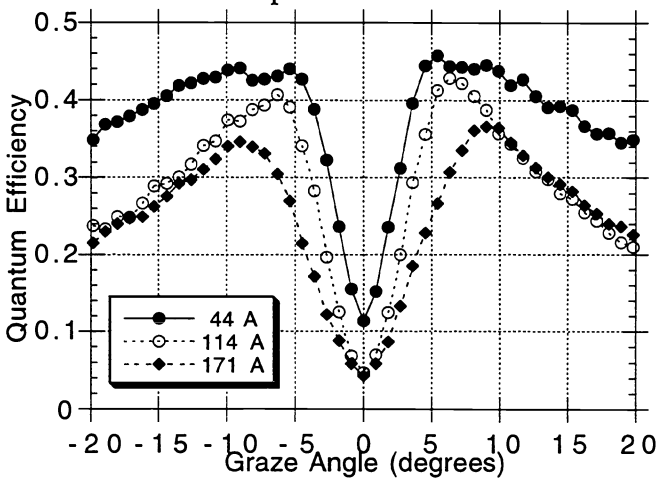

Figure 6. Quantum efficiency v.s. graze angle of incidence to the MCP pores for RbCl.

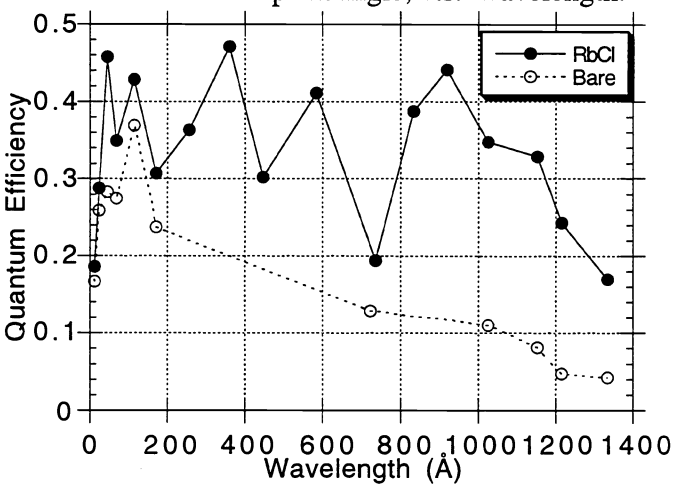

Figure 7. Quantum efficiency of RbCl & bare MCP measured at the peak angle, v.s. wavelength.

RbI material was measured twice, once with an evaporation angle of 11°, and then with a 3° deposition angle. The second RbI cathode was the better, as expected due to the greater penetration depth of the photocathode material into the pores. RbI QDE as a function of angle and wavelength are presented in Figures 4 and 5 respectively. RbI has a band gap of 6.1eV and electron affinity of ≈1.2eV, giving a photoemission threshold of ≈1700Å. It is hygroscopic, with a solubility of ≈150gm/cc, which is similar to CsI, but we have found that the handling requirements for RbI somewhat better than those for CsI. Photoemission data[9] also indicates that RbI should be a good photocathode material, with yields similar to RbBr [11]. The angular QDE response follows the normal pattern with the rapid drop in QDE at angles >5° due to grazing incidence reflection. The peak in the QDE at ≈114Å-171Å again correlates with the resonant peak in the absorption coefficient found at 95eV [10], although it is wider and lower QDE than CsCl as expected from the absorption coefficient data. The QDE cutoff at about 1700Å is apparent in Figure 5. The 2x bandpass QDE minimum at ≈800Å is more pronounced than CsCl. There are also the local maxima are found at ≈584Å and 1100Å , corresponding to one, and two photoelectron emission respectively.

RbCl QDE as a function of angle and wavelength are presented in Figures 6 and 7 respectively. RbCl has a band gap + electron affinity of ≈8.3eV, giving a photoemission threshold of ≈1500Å. RbCl is hygroscopic, with a solubility of ≈77gm/cc, which is similar to KBr, and the handling requirements do seem to be similar. Photoemission data[9] indicates that RbCl should be a good photocathode material, with yields similar to RbI. The angular QDE response is in accord with expectations, except that the 44Å curve is very flat at angles >5°, which is indicative of a short photoabsorption depth. There is no obvious short wavelength peak in the QDE, however. The resonant peak in the absorption coefficient is found at 150eV (≈80Å)[10], and is much smaller than either CsCl or RbI which may explain the absence of an obvious peak. The local maximum at ≈900Å is visible, but there are not enough data points to resolve any peaks between 200Å and 800Å.

4.2. CsI and BaCl photocathodes

Measurements for CsI and BaCl. photocathodes are shown in Figs. 8 & 9 respectively. CsI is a standard material among photocathodes, with many aspects of its performance in the literature[1,2]. CsI is included here as a comparison for the other materials as a reference baseline. The measurements obtained with the CsI cathode here are close to those obtained in our previous publication almost a decade ago[2]. CsI has a band gap of 6.3eV and an affinity of 0.1eV, giving a threshold wavelength of 1940Å. It is hygroscopic, with a solubility of ~100gm/cc. CsI has a high short wavelength QDE and because of its small band gap energy, has QDE that extends to longer wavelengths than the other alkali halides.

BaCl is more like MgF_2 than CsI. It has a band gap of <10eV giving a threshold wavelength of >1200Å, and a solubility of 40-60gm/cc. BaCl undergoes a phase transition before evaporation which may have some effect of the resulting cathode. BaCl produced a moderate improvement in QDE performance over a bare MCP, with ~25% QDE at 800Å vs ~12% for bare. However, it is interesting because the enhancement occurs between 400Å and 1300Å with a cutoff wavelength not much longer than a bare MCP. Thus for instruments which require QDE improvement in the EUV regime, with good rejection of FUV flux >1300Å, BaCl may be a good candidate photocathode material.

4.3. LiF, MgBr, and AgCl photocathodes

These materials produced photocathodes which actually decreased the QDE compared with bare MCP's. In the case of MgBr this can be partially attributed to hygroscopic behavior (see below). The band gaps for LiF, MgBr, and AgCl are 13.1eV, 10.65eV and ≈3.5eV respectively, giving photoemissive thresholds of 950Å, 1165Å and 3500Å respectively. Their QDE performance as a function of wavelength is shown in Fig. 10. The hygroscopic behavior of the first two materials is hard to estimate, but the solubilities are 0.27gm/cc for LiF, 100-120gm/cc for MgBr and 10^{-4} gm/cc for AgCl. LiF is quite good in terms of potential atmospheric exposure, compared to many other good

photocathodes. Its low QDE is due to a low photoemission yield[9]. MgBr has a reasonable level of solubility, and is comparable to NaBr and KI[8], however it seems to degrade much faster in air than the latter materials. The measurements made cannot be taken as representative of a fresh MgBr photocathode for this reason. AgCl has a very poor efficiency, and tends to discolor under exposure to visible light much like the other silver halides used for photographic film.

4.4. Hygroscopic behavior

Three of the materials were so hygroscopic that they deteriorated within seconds of exposure to atmospheric water vapor. These were MgBr, LiCl, and LiI. The MgBr merely discolored to a pale white color, indicative of the formation of hydrated globules of cathode material. LiCl and LiI "melted" into droplets within a short period after exposure to air at @40% relative humidity. Although LiCl and LiI have solubilities of 64gm/cc & 145gm/cc respectively, they behave far more severely than other materials with these solubility levels and cannot be used as photocathodes in "open face" MCP detectors.

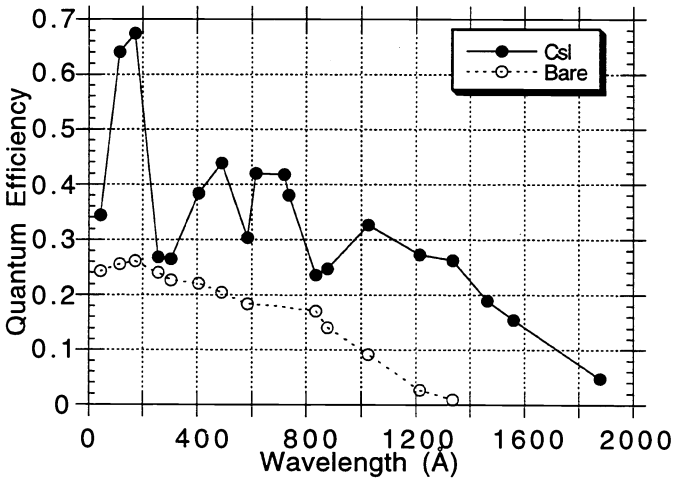

Figure 8. Quantum efficiency vs wavelength for CsI.

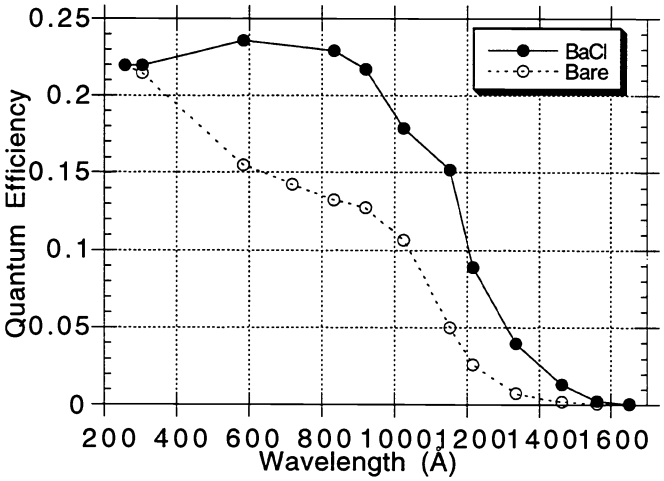

Figure 9. Quantum efficiency vs wavelength for BaCl.

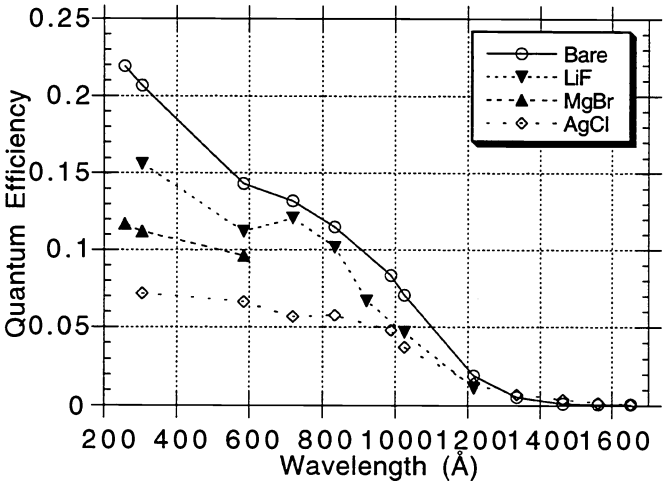

Figure 10. Quantum efficiency vs wavelength for three photocathode materials: LiF, MgBr, and AgCl.

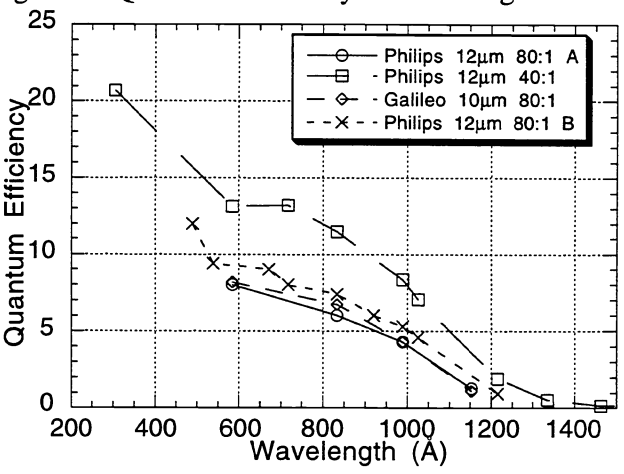

Figure 11. Quantum efficiency vs wavelength for various bare MCP's at 13° to the MCP pore axis.

4.5. Bare Microchannel Plate QDE Performance

Many measurements of bare MCP QDE have been made for different manufacturers and MCP types[12]. However, in most cases the QDE is very similar as can be seen in Figs. 3, 5, 7, 8, & 9. Over

the past few years we have noticed on a number of occasions that the QDE of some batches of MCP's that the QDE was significantly below that expected (Fig. 11). In addition it was found that the QDE of photocathodes deposited onto these MCP's was also low by a similar ratio. After a considerable amount of study we have surmised that the actual QDE of the photoemitting surfaces is probably not degraded. Cathodes produced at the same time on "normal" QDE MCP's were also normal. The problem is possibly due to inefficient detection of the emitted photoelectrons by the MCP (electron detection probability in Ref 3). We are currently attempting to resolve this problem with the manufacturers and will report on this at a future date.

5.0 KBr Photocathodes

5.1. KBr Lifetest

Our work with SOHO, EUVE, ALEXIS, ORFEUS and many other shuttle and rocket experiments has shown us that environmental degradation of photocathode performance can be a major concern. Detailed knowledge of cathode stability allows proper handling and storage of cathodes to be established, and long term operations in orbit predicted. Our lifetest studies include over 5.5 years for one KBr photocathode stored in N_2, showing about a 20% relative QDE degradation on average. In Figure 12, the QDE vs wavelength of the KBr lifetest detector at a 15° graze angle to the MCP pores is shown as a function of time. After an initial drop in QDE of ≈15% in the first year, the QDE has basically remained unchanged. The angular dependence of the QDE for KBr was also measured over time (Fig. 13). At 920Å the gradual drop in QDE is revealed, but the shape of the angle dependence essentially remains the same.

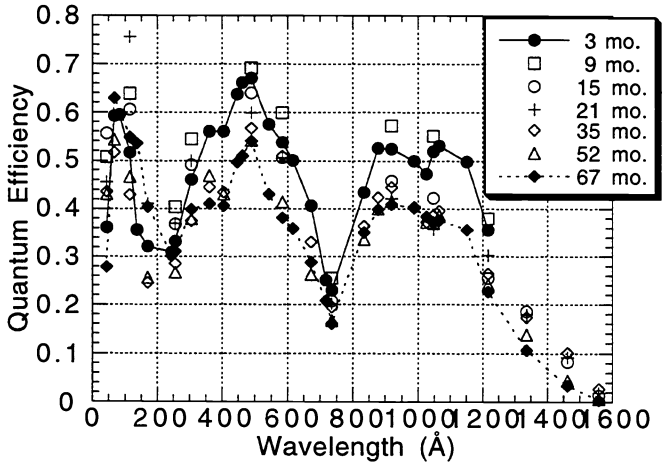

Figure 12. Quantum efficiency vs wavelength for the KBr lifetest detector measured over 5.5 years.

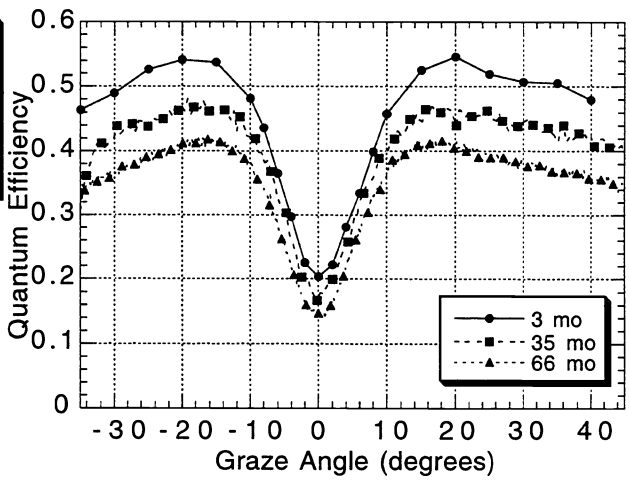

Figure 13. Quantum efficiency vs graze angle for the KBr lifetest detector at 920(Å) over 5.5 years.

Measuring the photoelectron number distributions and photoelectron energy spectra gives valuable information on the physical effects of cathode deterioration, such as photoelectron surface escape probabilities. A comparison of the photoelectron number distribution for the KBr lifetest detector at 68Å for many stages in the lifetest is presented in Figure 14. The photoelectron distribution is always dominated by the single photoelectron peak, but the initial measurement also has the highest two and three photoelectron peaks, and they are the most well defined. With increasing age, the two photoelectron peak becomes less intense as do the other multiple photoelectron peaks. At 66 months the two photoelectron peak is still clear but the three photoelectron peak has decreased dramatically. The photoelectron energy spectra of the KBr lifetest photocathode at 920Å is shown in Figure 15. The broad energy spectrum is a consequence of the dominance of single photoelectron emission at this wavelength, with potentially high values for the kinetic energy ($E\lambda - E_g - E_a \approx 6eV$). Very little happens to the

photoelectron energy distribution as the cathode ages, probably because these higher energy photoelectrons can easily escape the surface even when the photocathode is slightly degraded. (The offset in the energy distribution is due to a small residual field that penetrates the mesh grid).

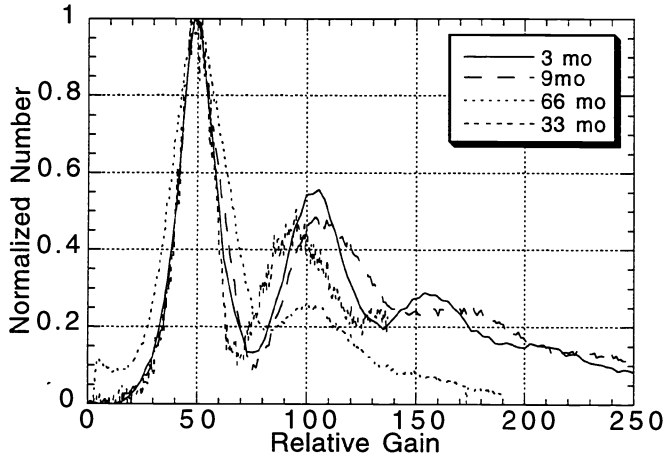

Figure 14. The photoelectron number distribution vs gain, $1e^-$, $2e^-$ etc, KBr lifetest detector @ 68Å.

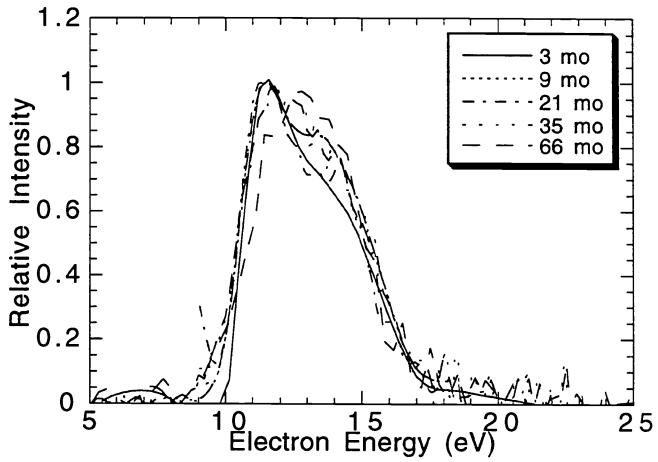

Figure 15. Photoelectron energy spectra for KBr lifetest detector at 920Å as a function of time.

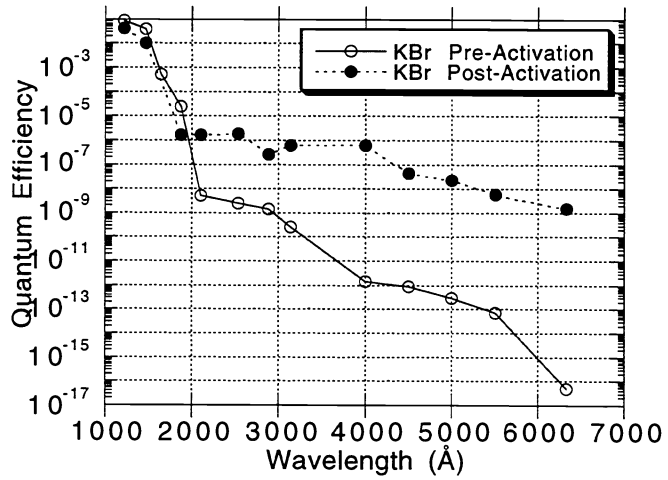

Figure 16. Quantum efficiency vs wavelength for KBr before & after full activation by 2537Å UV.

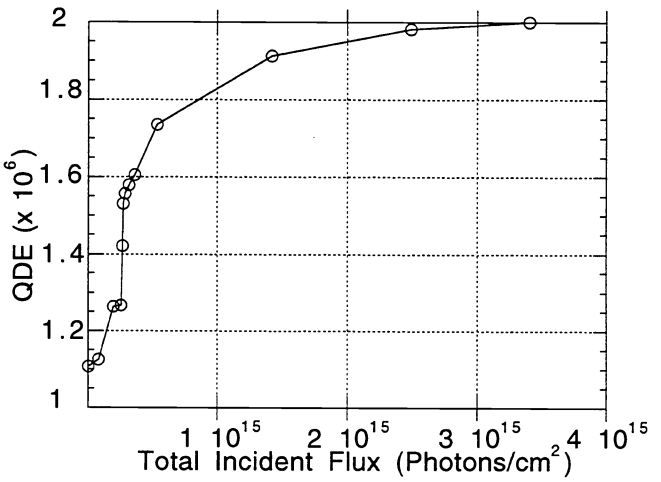

Figure 17. Increase in the 2537Å QE of KBr due to exposure with 2537Å photons.

5.2. KBr Activation

Although cathodes like KBr show good solar blindness, ($<10^{-12}$ @ 5000 Å) we have found that this can be degraded (QDE increased) after exposure to very high fluxes of UV or ions[13]. Any wavelength below ≈3000Å activates the cathode in a fairly short time (≈10 minutes for a Hg vapor lamp). Fig.16 shows the typical activation curve for 2537Å, with QE's at wavelengths below 2000Å hardly affected, and those at longer wavelength enhanced by factors of >five orders of magnitude. Deactivation can be accomplished by re-exposure to air, or illumination with strong visible (laser) illumination. The activated QDE @ 5000Å seems to level off at $\approx 10^{-8}$ QDE, possibly when all the available energy levels are fully populated. The rate of activation is illustrated in Fig. 17 by comparing the QE of the cathode as a function of incident flux. Although the integrated flux is high, this is because the QDE at the activation wavelength is very low. If the cathode were activated by a shorter wavelength source, where the QDE is

higher, the integrated flux requirement may be considerably smaller. This could be a serious problem for instruments with high input flux levels, and where the scattered light and the background levels need to be very low. Our investigations have also established rate constants for activation and deactivation of KBr which will be presented elsewhere. A tentative model of the process is that inter-band gap metastable energy states are being populated by the activation. These higher states can then photoemit when stimulated by long wavelength UV. Other cathode UV materials probably have the same basic problem, and we are investigating some of the more common photocathodes for the effect.

6.0 REFERENCES

1. E.B. Saloman, J.S. Pearlman and B.L. Henke, "Evaluation of high efficiency CsI and CuI photocathodes for soft x-ray diagnostics", Appl. Opt., Vol. 19 (5), 749-753, 1980.

2. O.H.W. Siegmund et al., "High quantum efficiency opaque CsI photocathodes for the extreme and far ultraviolet", Proc SPIE, Vol. 687, 117-124, 1986.

3. O.H.W. Siegmund et al., "Ultraviolet quantum detection efficiency of potassium bromide as an opaque photocathode applied to microchannel plates," Appl. Opt., Vol. 26, 3607, 1987.

4. O.H.W. Siegmund et al., "Soft x-ray and extreme ultaviolet quantum detection efficiency of potassium bromide photocathode layers on microchannel plates," Appl. Opt., Vol. 27, 1568, 1988.

5. O.H.W. Siegmund, K. Coburn and R.F. Malina, "Investigation of large format microchannel plate Z configurations," IEEE, Trans. Nucl. Sci. NS-32, 443, 1985.

6. C. Martin et al., "Wedge-and-strip anodes for centroid-finding position sensitive anodes and particle detectors," Rev. Sci. Insrtum., Vol. 52 (7), 1067-1074, July 1981.

7. O.H.W. Siegmund and G.A.Gaines, "Photoelectron energy spectra of opaque photocathodes in the extreme and far ultraviolet," Proc SPIE, Vol 1344, 217-227, 1990.

8. D.R. Marsh, O.H.W. Siegmund and J. Stock, "Progress on high efficiency photocathodes for soft x-ray, EUV and FUV photon detection," Proc SPIE, Vol. 2006, 51, 1993.

9. P. Metzger, "On the quantum efficiencies of twenty alkali halides in the 12-21 eV region," J. Phys. Chem. Solids, Vol.26, 1879, 1965.

10. DESY, Optical properties of some insulators in the vacuum ultraviolet region (1977)

11. O.H.W. Siegmund, and G. Gaines, "Extreme Ultraviolet quantum detection efficiency of rubidium bromide opaque photocathodes", Applied Optics, 29 (31), 4677-4685 (1990)

12. G.W. Fraser, J.E. Lees, J.F. Pearson, A.P. Nichols, P. Bailey, "Near edge structure in the soft X-ray quantum efficiency of microchannel plate detectors", Proc SPIE, Vol. 2280, 101, 1994

13. O.H.W. Siegmund et al., "Microchannel plates for the UVCS and SUMER instruments on the SOHO satellite," Proc SPIE, Vol. 2518, 344, 1995